Available online at www.sciencedirect.com

ScienceDirect

Procedia CIRP 102 (2021) 115–120

www.elsevier.com/locate/procedia

18th CIRP Conference on Modeling of Machining Operations

Finite element simulation of sintering of metal-bonded grinding wheels

Denkena, B[a], Krödel, A, Liu, Y, Kempf, F, Kostka, M*

[a]*Institute of Production Engineering and Machine Tools (IFW), Leibniz Universität Hannover, Germany*

* Corresponding author: Mateus Kostka Tel.: +49-511-762-18357; fax: +49-511-762-5115. *E-mail address:* Kostka@ifw.uni-hannover.de

Abstract

The grinding wheel properties porosity, particle distribution and the grain holding force influence the surface roughness of the machined workpiece and the performance of the grinding process. These properties of a grinding wheel are in turn defined during tool production. However, the adaptation of the properties of a grinding wheel to the specific grinding task is currently based on empirical knowledge and experience. Understanding the interdependencies from the initial manufacturing to the final grinding results is the key to achieve the target-oriented generation of the grinding wheel properties for the grinding task at hand. With regard to the large number of powder particles for the manufacturing of metal-bonded grinding wheels, an analytical investigation of the powder metallurgical processes is not suitable. Numerical simulations offer a cost and time saving alternative to provide information on the sintering behavior and gain knowledge on the acting mechanism. In this article the sintering of a metal-bonded diamond grinding wheel is modelled and the obtained results are connected to material properties of the resulting grinding layer.

Keywords: Simulation, Sintering, Metal-bonded grinding wheels

1. Introduction

The manufacturing process of grinding wheels has a great influence on their application behavior. The abrasive wear resistance as well as the toughness and brittleness of the bond can be adjusted via the bond composition and the manufacturing parameters [1]. A deeper understanding of the manufacturing process of grinding wheels inevitably provides the basis for a better understanding of the grinding process. Characteristic values, which are set by the manufacturing process, have an influence on the resulting properties, such as porosity or critical bond stress and thus also on the actual grinding process [2].

The most common production process for sintered metal-bonded grinding wheels is hot pressing, which includes the steps of mixing, filling, pressing and sintering [3]. The tool's wear resistance and the toughness of the bond as well as its hardness can be changed both by bond composition and sintering parameters [4]. Concerning the latter, temperature and time are the dominant variables. Furthermore, sintering pressure and grain size of the used metal powders are of influence [5]. Lin shows that the sintering temperature has a greater influence on the grinding behavior of vitrified grinding wheels than the holding time [6]. For hot-pressed metallic bonded diamond grinding wheels, Kühl reports an influence of the sintering parameters comparable to that of vitrified grinding wheels, where the influence of temperature has the greatest impact on the resulting grinding wheel properties [7]. According to these two sources, there is an optimal sintering temperature which leads to the highest grinding layer density and the highest grain retention forces [6].

With regard to the large number of powder particles, an analytical investigation of the powder metallurgical processes is not suitable. Numerical simulation offers a cost and time saving alternative. The Discrete Element Method (DEM) is a useful tool for the simulation of mixing and filling processes with regard to the material properties and the kinematics of the particles [8]. On the other hand, the finite element method

10.1016/j.procir.2021.09.020

predicts precisely the deformations and stresses acting within the particle [9]. To combine the strength of these two methods, the simulation of the process chain with the help of DEM and FEM simulation is developed and introduced in this article.

2. Simulation of the process chain

In the process chain (Figure 1) the particle number, size distribution and material properties of bronze powder and diamond grain serve as input variables for the simulation. Within the simulation of the process chain, the DEM simulation is used for mixing and filling processes and the FEM simulation for pressing and sintering. The simulation is used to calculate the grain distribution and porosity as well as the residual stresses in the grinding layer.

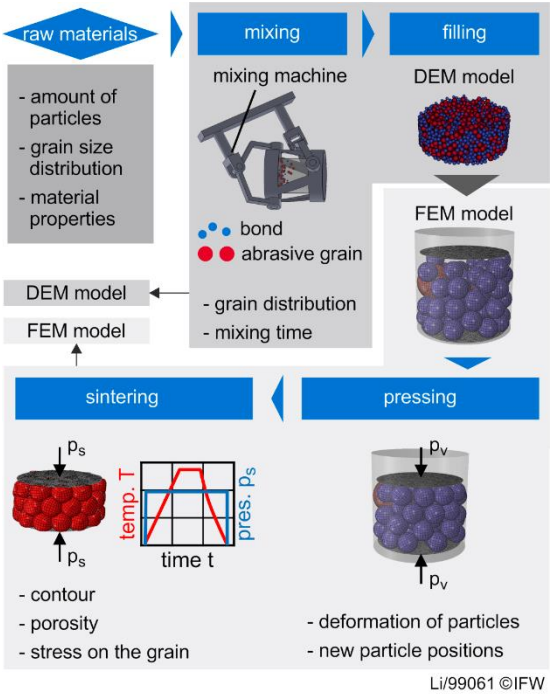

Figure 1: Simulation of the process chain for the production of sintered metal bonded grinding tools

The resulting residual stresses in the grinding layer after cooling and shrinkage are important for the later behavior of the bond. They have a significant influence on the mechanical properties of the bond, for example the critical bond stress and thus influence the behavior of the tool during grinding. The critical bond stress serves as an evaluation criterion for the mechanical properties of the grinding layer. As a macroscopic quantity, it is a measure of the cohesion of the entire grinding layer and thus also influences the wear susceptibility. This, in turn, has an influence on the ability of the grinding layer by being sharpened, and as a result, also on the application behavior of the grinding wheels [14].

In this study, the manufacturing process of bronze bonded diamond grinding wheel is investigated. The powder material for the bond system is pre-alloyed bronze with 20% tin content and 40 µm grain size. The size of diamond grains in the shape of truncated octahedron is 76 µm. In the DEM simulation, a model of the mixing machine WILLY A. BACHOFEN Type T2A is built up based on a CAD drawing. The kinematics of the mixing machine are detected and rebuilt in the DEM simulation system "LIGGGHTS". The particles are moved in the cylindrical container, which follows the kinematic of the mixing machine. The Hertz–Mindlin contact model is used for the simulation [10]. In this contact model, the interactions among the grains and between the grains and wall are considered as a spring-dashpot in the normal and tangential directions to their lines of centers. The material properties, such as Young's modulus, Poisson ratio, friction coefficient between grains as well as friction coefficient between grains and inner wall of the container are taken from references [11–13]. With the help of the DEM simulation the position of every particle is calculated at each simulation time step. This output allows the investigation of the grain distribution during the processing and the necessary mixing time [14].

The grain distribution is also an important input for the FEM simulation of mixing and pressing. The FEM simulations are conducted in the FEM software ABAQUS. To ensure the continuity of the process chain and the consistency of the data flow, an interface between DEM and FEM simulations is developed. Through the interface, the data about the size and position of each particle from the DEM simulation are read out as input variables for the FEM simulation. With these data the input script for the model construction in ABAQUS is automatically generated. The particles in the FEM model have the same size and position as in the DEM model.

In the pressing process, the particles are pre-compressed through a pressure of p_p = 3.68 MPa at room temperature. In the experimental pressing process, 14.9 g mixture is compressed into a cylinder with the diameter of 22 mm and a height of 10.97 mm. Thus, the density of the compressed the mixture after pressing process is 3.57 g/cm^3.

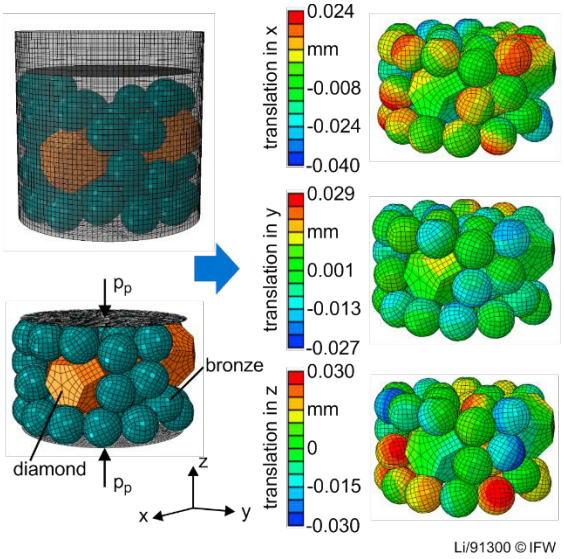

Figure 2: FEM simulation of the pressing

To simplify the simulation and shorten the simulation time, 56 particles from the DEM simulation are used for the following FEM simulation. They are 54 bronze particles with the

diameter of 40 µm and 2 diamond grains with the size of 76 µm, by which the grain concentration is C = 25 V%. The simulation model in ABAQUS is shown in Figure 2. The gray cylinder around the particles represents the mold. The gray disks work as punches. The mold and the punches are set as rigid bodies. The mold is fixed, while the punches have only one-degree freedom of movement in the direction of the z axis. The particles have all six degrees of freedom for movement. The interaction between the bodies is defined using general contact as all with self. Thus, the particles are able to be pushed towards to or away from another. The compression load will be transported through the contact surfaces and result in the elastic as well as plastic deformation of the particles. Figure 2, right, shows the translation of the particles in x, y and z direction. Due to the pressure the particles are displaced. The largest displacement of the particles is 0.04 mm in x-direction, 0.029 mm in y-direction and 0.03 mm in z-direction. The end density of the mixture from the simulation is 3,63 g/cm^3, which is only 1.7% lower than the experimental value. The relative positions between the particles are changed. For example, the distance between the centers of the diamond grains is increased from 0.098 mm to 0.112 mm. The positions of the particles are important input variables for the subsequent simulation of sintering, since the relative positions of the diamond grains and the bond particles influence the porosity in the grinding layer and the mechanical stresses on the diamond grain.

After the pressing at room temperature the mold and the mixture are hot sintered in a “Dr. Fritsch DSP 510” sintering press, employing FAST (Field Assisted Sintering Technology) [15]. The hot sintering process consists of the three phases heating, holding and cooling (Figure 3). The total time of the process results from the partial times of the three phases. While the time from the second phase results directly from the selection of the holding time, the times of the heating or cooling phase depend on the selected heating or cooling rate and the maximum temperature to be reached. A reduction of the production time is thus possible by using low sintering temperatures and high heating rates. In this study, the sintering process is conducted with a pressure of 35 MPa at the temperature of 620 °C. Thus, this pressure and sintering temperature are also used in the further simulation for the sintering.

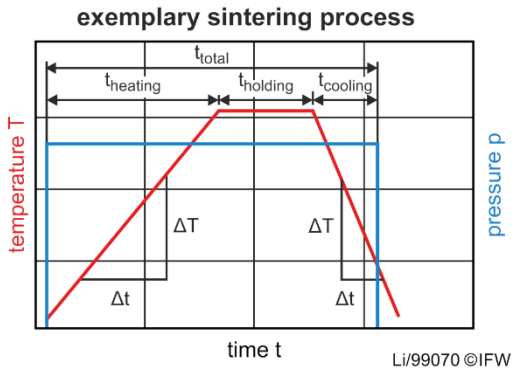

Figure 3: Temperature and pressure during the sintering process

Since the mixture is deformed at a high temperature, the material properties at such temperature is necessary as input for the simulation. Due to the fact that the strength of diamond remains approximately constant at this temperature [16], the mechanical flow behavior of bronze is to be measured and determined.

3. Experimental determination of material properties at high temperature and simulation verification

In this study, the characterization of mechanical flow behavior of bronze was carried out on a quenching and forming dilatometer DIL805 A/D+T from TA Instruments (former BÄHR Thermoanalysis). The dilatometer allows the performance of precise heat treatments on cylindrical specimens, which can be interrupted at any time and completed by upsetting tests. A schematic illustration of the measurement setup for carrying out thermomechanical analyses in the forming dilatometer is shown in Figure 4.

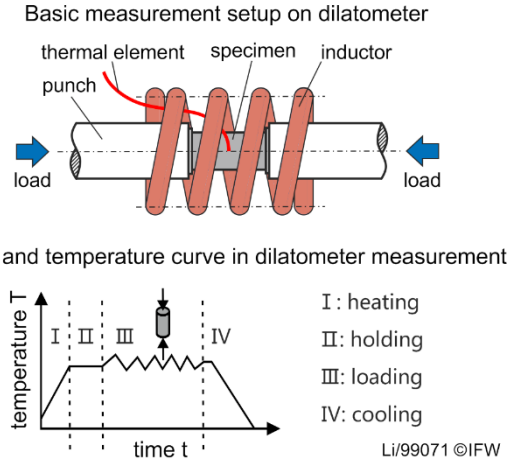

Figure 4: Basic measurement setup for the thermomechanical analyses on the dilatometer DIL 805 A/D+T

As can be seen in Figure 4, a cylindrical specimen is positioned between two punches in the test chamber of the dilatometer, which can transmit forces to the specimen. The specimen is clamped almost without load by an integrated spring mechanism of the measuring system. While one of the stamps can be moved at a defined speed by a hydraulic module for force transmission, the second stamp acts as a counter support.

The entire test chamber of the dilatometer can be evacuated or filled with protective gas via a connected pump system before heat treatment is carried out. The actual heat treatment of the specimen is carried out by a double-walled induction coil, which concentrically surrounds the specimen and thus ensures a heat development as homogeneous as possible. By generating an alternating magnetic field, eddy currents are induced in the material to be examined without contact. Due to the electrical resistance of the metallic specimen, a part of the introduced power is converted into heat. The specimen is heated in a defined manner by the losses associated with the current flow.

For the tests cylindrical specimen with a diameter of d = 5 mm and a length of L = 10 mm that consist of pre-alloyed bronze

with 20% tin content are produced. To investigate the deformation behavior of specimens at different temperature, the specimens are heated to 340 °C, 520 °C und 620 °C, and loaded with a force of 700 N. Thus, the pressure at the beginning of the measurement is 35 MPa. The length changes of the specimens are shown in Figure 5.

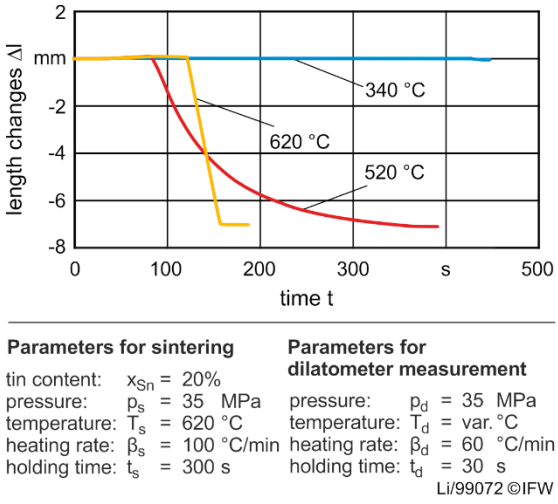

Figure 5: Length changes of the specimens in the dilatometer measurement

Between the reaching of the target temperature and the loading of the force, the specimens are held at the target temperature for 300 s. The thermal expansion ΔL in the length direction of the specimens is measured by the length changes, which are positive. The thermal expansion ΔL is 0.033 mm at 340 °C, 0.087 mm at 520°C and 0.106 mm at 620 °C. The thermal expansion coefficient can be calculated according to equation 1.

$$\alpha_L = \frac{\Delta L}{L \cdot \Delta T} \quad (1)$$

Thus, the thermal expansion coefficient at 340 °C, 520 °C and 620 °C is $1.03 \cdot 10^{-5}$/°C, $1.74 \cdot 10^{-5}$/°C and $1.76 \cdot 10^{-5}$/°C respectively.

In order to assess the flow behavior, the recorded curves of force and length changes are converted into stress-strain curves, which are shown in Figure 6.

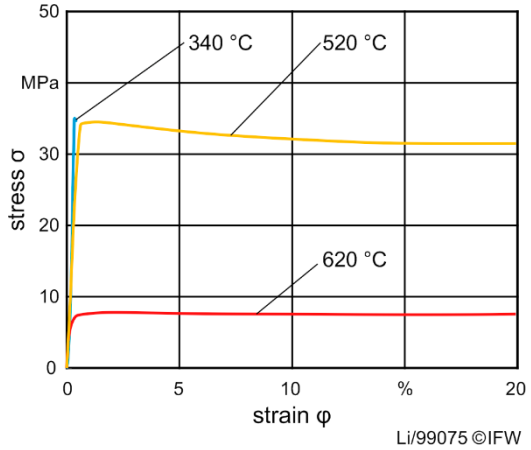

Figure 6: Stress-strain curves of bronze at different temperatures

At 340 °C the bronze only shows elastic deformation under the pressure of 35 MPa. The Young's modulus E is calculated from the ratio of stress σ to strain φ, which is 95 GPa at 340 °C. By reaching the temperature of 520 °C the specimen is thermally softened and deformed plastically under the load. It shows a Young's modulus of 65 GPa and a yield stress of 34 MPa. At the temperature of 620 °C the yield strength of the specimen is further reduced to 7.5 MPa and the calculated Young's modulus is 24 GPa. The measurements at 520 °C and 620 °C are compulsively stopped before reaching the presupposed loading time at the length changes of 7 mm, in order to protect the equipment by stopping on the safe position. These thermomechanical properties are given as input in the model for the sintering simulation.

4. Sintering Simulation

With the input of material properties gained from the dilatometer measurements, the sintering simulation is conducted as the next step of pressing simulation. As shown in Figure 7, the particles are heated to the target temperature and a pressure of 35 MPa, which is the same as the pressure in the exemplary sintering process, is loaded by the punches.

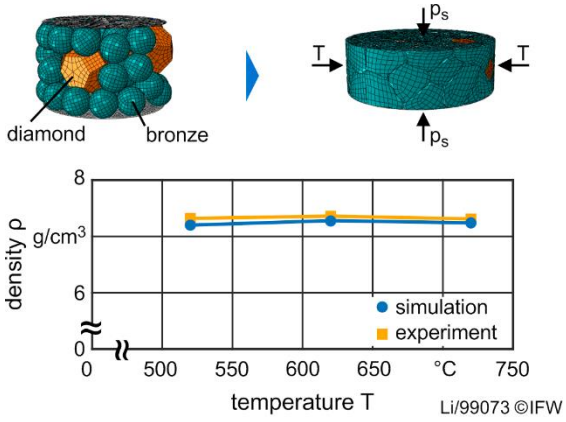

Figure 7: Simulation of the sintering process and the density after cooling

The results from the sintering simulation are used to investigate influences of the sintering temperature on the resulting properties of the grinding layer. For this purpose, sintering simulations with the temperature of 520 °C, 620 °C and 720 °C are conducted with the same model. In the simulation the density of the specimen after cooling is calculated and shown by the blue curve in Figure 7. The yellow curve represents the experimentally measured density of specimens, which are also sintered at 520 °C, 620 °C and 720 °C. Both the simulation and the experiment show that the density of the specimen is not significantly influenced by the sintering temperature. The biggest deviation between the values from simulation and experiment is 1.6% at 520 °C.

Furthermore, the bond residual stress is determined to characterize the critical bond stress of the grinding layer. Figure 8 shows the residual stress distribution in a cross section, which is parallel to the x-y-plane. In this simulation, the sintering temperature is 520 °C and the shown status of the specimen is after cooling. Thereby, the distribution of residual stresses in

all three coordinate directions is evaluated. It is shown that in the most areas of the section compressive stress is generated. In all of the three directions the maximum tensile residual stress appears close to the diamond grains. They are $\sigma_{x,max}$ = 199.92 MPa, $\sigma_{y,max}$ = 195,69 MPa and $\sigma_{z,max}$ = 196.63 MPa. The average values of residual stress in the three directions are compressive, they are $\sigma_{x,ave}$ = -58.33 MPa, $\sigma_{y,ave}$ = -58.03 MPa and $\sigma_{z,ave}$ = -52.12 MPa. The stress distribution from the simulation with the sintering temperature of 620 °C and 720 °C is shown in Figure 9.

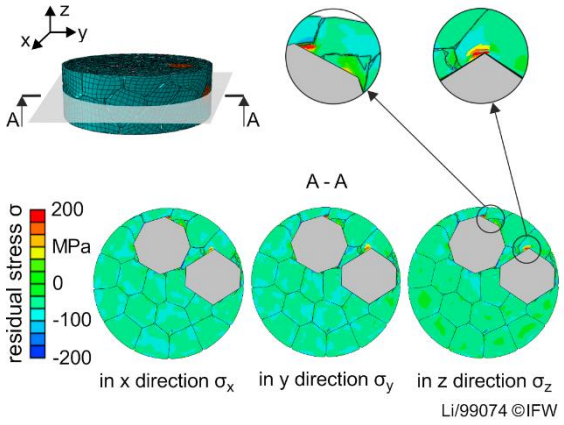

Figure 8: Residual stress distribution from the simulation with 520 °C after cooling

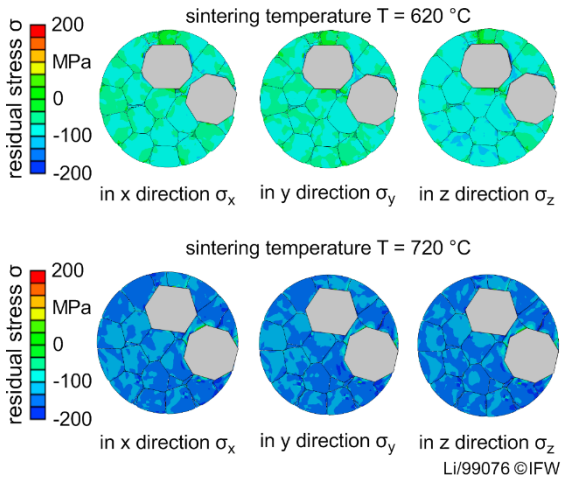

Figure 9: Residual stress distribution from the simulation with 620 °C and 720 °C after cooling

In all of the three directions lower maximum tensile stress and higher compressive stress as average stress in all areas are generated by sintering with 620 °C and 720 °C. The maximum tensile residual stress σ_{max} and the average residual stress σ_{ave} are listed in Table 1.

Table 1: Maximum tensile residual stress σ_{max} and average residual stress σ_{ave} from simulation with different sintering temperatures

Stress [MPa]	Sinter temperature [°C]		
	520 °C	620 °C	720 °C
$\sigma_{x,max}$	199.92	152.42	102.62
$\sigma_{y,max}$	195.69	151.86	115.13
$\sigma_{z,max}$	196.63	146.82	105.86
$\sigma_{x,ave}$	-58.33	-71.70	-135.58
$\sigma_{y,ave}$	-58.03	-70.28	-134.70
$\sigma_{z,ave}$	-52.12	-81.90	-135.40

The specimen with higher maximum tensile stress and lower average compressive stress is likely to fail with a lower critical bond stress, because cracks can easier penetrate through the bond. Thus, the critical bond stress of the specimens sintered at 520 °C should be the lowest, while the highest critical bond stress is to be shown by the specimen with the sintering temperature of 720 °C. This corresponds to the experimentally determined influence of sintering temperature on critical bond stress [14], the critical bond stress rises with increasing sintering temperature. The occurring stress within the specimen cannot be measured experimentally due to the high pressure, high temperature and lack of accessibility during the sintering process. The simulation, however, enables to identify the stress in the grain-bond interface, which influences the interface properties and thus the grain holding forces. Consequently, an optimized formation of the grain-bond interface between the diamond and the bronze particles improves the application behavior of the manufactured grinding wheel, e.g. tool wear.

Besides the critical bond stress the porosity is also investigated by using this simulation. Metallic bonded grinding wheels are known for a dense body exhibiting minor porosity. However, usually there is in fact some pore volume content. The field output variable EVOL in ABAQUS enables the calculation of the current element volume in the model. By adding the volume of every element, the volume of the solid part V_s can be obtained at the end step of the simulation. The total volume of the specimen V_t can be calculated as a cylinder. The diameter of the cylinder is same as the mold, and the height is the distance between the two punches. The porosity Φ can be calculated according to equation 2.

$$\Phi = 1 - \frac{V_s}{V_t} \quad (2)$$

In experiment, the porosity of the grinding layer specimens is determined by comparing the theoretical density ρ_{th} of the grinding layer with its actual density ρ. Its actual density ρ can be obtained via Archimedes' principle by submerging a sample in water and measuring its buoyancy. In this method, the porosity Φ is calculated using equation 3.

$$\Phi = 1 - \frac{\rho}{\rho_{th}} \quad (3)$$

The porosity from the simulation at different sintering temperature is shown by the blue curve in Figure 10. The yellow curve represents the experimentally measured porosity of grinding layer specimens, which are sintered at 520 °C, 620 °C and 720 °C.

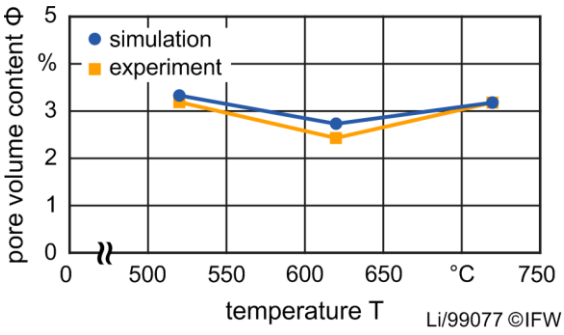

Figure 10: Residual porosity with different sintering temperatures

Both simulation and experiment show the same development tendency of the porosity with rising sintering temperature and are therefore in good agreement. A quantitative evaluation of the pore volume is, however, due to measurement inaccuracies of the experimental data of about 0.5 % not possible. However, a qualitative evaluation of the data is still reasonable. Within the grinding layer of a bronze bonded grinding wheel small pores do not significantly improve the effect of the coolant due to capillary action. However, each pore can be seen as an interruption of the bond which leads to a decrease in overall adhesion inside the grinding layer.

5. Conclusion and outlook

In the first part of this article, a simulation model of the process chain for the production of sintered metal bonded grinding tools has been presented. Within the simulation of the process chain, the DEM simulation is used for mixing and filling processes and the FEM simulation is used for pressing and sintering. Between the DEM and FEM simulation, an interface is developed to read the output data of the DEM simulation and to generate the input script for the FEM simulation. By means of this interface, the sintering simulation can be conducted with the same particle size and distribution as the DEM simulation. In order to obtain the material properties of the bond for the sintering simulation, dilatometer measurements are conducted. Through the sintering simulation, residual stress and residual porosity in the grinding layer after cooling are calculated. The results show that both tensile and compressive stresses are generated. The grinding layer is dominated by the compressive stress and the average stress of the whole specimen is compressive. With sintering temperature increases from 520°C to 720 °C, lower maximum tensile stress is generated, while the absolute value of the average stress (compressive) is higher. This corresponds to a higher critical bond stress with increasing sintering temperature. The residual porosity of samples decreases as the sintering temperature increases from 520 °C to 620 °C, and increases as the sintering temperature increases from 620 °C to 720 °C.

Since the diffusion of the pre-alloyed bronze particles is not considered in this simulation, which must happen in reality, sintering simulation with the consideration of diffusion will be investigated and evaluated in future research.

Acknowledgement

The authors thank the "Lower Saxony Ministry of Science and Culture" for their financial support within the project "Fundamentals of model-based design and production of grinding wheels".

References

[1] Klocke, F.: Manufacturing Processes, Vol. 2, Springer, 2009.

[2] Denkena, B., Grove, T., Bremer. I., Behrens, L.: Design of bronze-bonded grinding wheel properties, CIRP Annals, Vol. 65, 2016, p. 333-336.

[3] Denkena, B., Grove, T., Göttsching, T., Dzierzawa, P., Kempf, F.: Methods of analysis for a deeper understanding of the grinding process, Advances in Abrasive Technology, 2017, p. 945-951

[4] Weber, G., Weiß, C.: DIAMIX – Eine Bindungsfamilie auf Basis von DIABASE-V21, Industrie Diamanten Rundschau, 39, 2005, p. 134 – 138.

[5] Tillmann, W., Kronholz, C.: Verschleißuntersuchungen an Diamant-Metall-Verbunden zur Realisierung eines trockenen Bearbeitungsprozesses, 6. IFW-Steinkolloquium, Entwicklung in der Naturstein- und Bauwerkstoffbearbeitung, 12.-13. November 2008, Hannover, Germany, Berichte aus dem IFW, 09:69-77.

[6] Lin, K.-H., Peng, S.-F., Lin, S.-T.: Sintering Parameters and Wear Performances of Vitrified Bond Diamond Grinding Wheels, International Journal of Refractory Metals & Hard Materials, 25, 2007, p. 25-31.

[7] Kühl, C.: Freies Sintern – Admix FS 0100 eine preiswerte Alternative zum konventionellen Heißpressen, Dihw, 04/2010, p. 54-58

[8] Cleary, P.W.: DEM Simulation of Industrial Particle Flows: a Case Studies of Dragline Excavators, Mixing in Tumblers and Centrifugal Mills, Powder Technology, 109, 2000, p. 83-104.

[9] Zienkiewicz, O.C., Taylor, R.L., Fox, D.: The Finite Element Method for Solid and Structural Mechanics, Butterworth-Heinemann, Oxford, 2014.

[10] Chand, R., Khaskheli, M.A., Qadir, A., Ge, B.L., Shi, Q.F.: Discrete Particle Simulation of Radial Segregation in Horizontally Rotating Drum: Effects of Drum-length and Non-rotating End-plates. Physica A 391, 2012, p. 4590–4596.

[11] Simon, N.J., Drexler, E. S., Reed, R.P.: Properties of Copper and Copper Alloys at Cryogenic Temperatures, NIST Monograph 177, National Institute of Standards and Technology, Sponsored by International Copper Association, Ltd. 708 Third Avenue, New York, NY 10017, 1992.

[12] Gercek, H.: Poisson's Ratio Values for Rocks. International Journal of Rock Mechanics and Mining Sciences 44(1), 2007, p. 1–13.

[13] Straffelini, G.: Friction and Wear: Methodologies for Design and Control, Springer International Publishing, Switzerland, 2015.

[14] Denkena, B., Grove, T., Kempf, F., Dzierzawa, P., Bouabid, A., Liu, Y.: Model-based manufacturing and application of metal-bonded grinding wheels, CIRP Annals, Vol. 68, Issue 1, 2019, p. 321-324.

[15] Denkena, B., Grove, T., Göttsching, T., Dzierzawa, P., Kempf, F.: Methods of analysis for a deeper understanding of the grinding process, Proceedings of the 20th International Symposium on Advances in Abrasive Technology, ISAAT 2017, 3-6 December 2017, Okinawa, Japan, p. 945-951.

[16] Weidner, D.J., Wang, Y., Vaughan, M.T.: Strength of Diamond, Science, Vol. 266. Issue 5184, 1994, p. 419-422.